CCFE
CULHAM CENTRE FOR FUSION ENERGY

UK Atomic Energy Authority

UKAEA-CCFE-PR(25)403

M. Maslov, E. Lerche, C. Angioni, F. Auriemma, C. Bourdelle, E. Bray, A. Dal Molin, A. Kappatou, D. Keeling, D.B. King, J. Lombardo, R. Lorenzini, J. Mailloux, M. Marin, I. Monakhov, M. Nocente, M. Poradzinski, D. Rigamonti, M. Siccinio, M. Tardocchi, JET contributors, WPTE contributors.

Insights of the JET high fusion power scenario in the final DT campaign

Insights of the JET high fusion power scenario in the final DT campaign

M. Maslov, E. Lerche, C. Angioni, F. Auriemma, C. Bourdelle, E. Bray, A. Dal Molin, A. Kappatou, D. Keeling, D.B. King, J. Lombardo, R. Lorenzini, J. Mailloux, M. Marin, I. Monakhov, M. Nocente, M. Poradzinski, D. Rigamonti, M. Siccinio, M. Tardocchi, JET contributors, WPTE contributors.

This is a preprint of a paper submitted for publication in Plasma Physics and Controlled Fusion

Insights of the JET high fusion power scenario in the final DT campaign

M. Maslov[1], E. Lerche[2], C. Angioni[5], F. Auriemma[3], C. Bourdelle[4], E. Bray[10], A. Dal Molin[6], Z. Huang[1], A. Kappatou[5], D. Keeling[1], D.B. King[1], J. Lombardo[3], R. Lorenzini[3], J. Mailloux[1], M. Marin[8], S. Menmuir[1], I. Monakhov[1], M. Nocente[6,7], M. Poradzinski[9], D. Rigamonti[6], M. Siccinio[5], M. Tardocchi[6], JET contributors[11] and WPTE team[12]

[1]*UKAEA, Culham Campus, Abingdon OX143DB, United Kingdom of Great Britain and Northern Ireland*
[2]*Laboratory for Plasma Physics, ERM/KMS, B-1000 Brussels, Belgium*
[3]*Consorzio RFX CNR-ISTP, Corso Stati Uniti 4, 35127 Padova, Italy*
[4]*CEA, IRFM, F-13108 St-Paul-Lez-Durance, France*
[5]*Max-Planck-Institut für Plasmaphysik, Boltzmannstr. 2, 85748 Garching, Germany*
[6]*Institute for Plasma Science and Technology, CNR, via Cozzi 53, 20125 Milan, Italy*
[7]*Department of Physics, University of Milano-Bicocca, Piazza della Scienza 3, 20126 Milan, Italy*
[8]*EPFL, Swiss Plasma Center (SPC), CH—1015 Lausanne, Switzerland*
[9]*Institute of Plasma Physics and Laser Microfusion, Hery 23, 01-497 Warsaw, Poland*
[10]NEMO group, Dipartimento Energia, Politecnico di Torino, Italy
[11]see the authors list of C.F. Maggi et al., Nucl. Fusion 64 (2024) 112012
[12]see the authors list of E. Joffrin et al., Nucl. Fusion 64, (2024) 112019

Abstract: In its lifetime of around 40 years of scientific operations, Joint European Torus (JET) has performed three full-scale DT experimental campaigns: one in 1997 (DTE1) and two more in a relatively quick succession in 2021 (DTE2) and 2023 (DTE3). One of the goals of these campaigns, apart from studying a variety of physics effects relevant to DT plasmas, was demonstration of fusion power at large scale compatible with JET specifications. The focus was also made on the sustainability of the plasma, i.e. ability to keep the fusion power at high amplitude for extended duration of time: 5 seconds, matching the engineering limits of JET. This was found to be especially challenging after tungsten plasma facing components were implemented during the ITER-like wall upgrade in 2009-2011. In DTE2 the highest performing plasma (from the released fusion power point of view) has demonstrated E_{fus}=59MJ of fusion energy from a single discharge. The fusion power averaged over 5 seconds interval was $<P_{fus}>_{5s}$=10.1MW. In the final DT campaign DTE3 the scenario performance has been extended to E_{fus}=69MJ from a single discharge and $<P_{fus}>_{5s}$=12.4MW. The average fusion power generation efficiency averaged over the same period was $<Q>_{5s}=<P_{fus}>/<P_{in}>$=0.36. The main goal of the additional high fusion power pulses in DTE3 was to demonstrate better sustainability of the discharges, as in all cases in DTE2 where the maximum fusion power was reached, the plasmas suffered from core impurity accumulation. This was only partially successful, as the progressive cooling down of the plasma core due to excessive core radiation could not be avoided, but was slowed down sufficiently to demonstrate significantly higher $<P_{fus}>$ over the desired 5 second period.

1. Introduction

Future magnetic confinement fusion plants will be generating power from thermonuclear reactions which will take place in a close to 50/50 D-T mixture plasmas with ion temperatures up to at least T_i~20keV and density as large as attainable, n_e~$10^{20}m^{-3}$ or higher. This parameter combination has never been achieved in the present-day machines, and only two tokamaks so far, TFTR and JET, were able to do experiments with D-T fuel mix. ITER is expected to be the first burning plasma experiment with the fusion power generation efficiency, $Q=P_{fus}/P_{in}$~10. ITER operations are currently expected to begin in 2035 [1].

For the fusion machines which cannot routinely achieve efficient thermonuclear burn conditions, a significant proportion of generated fusion power can come from so-called beam-target reactions, those between relatively cold (T~5-10keV) plasma ions and suprathermal ions which resulted from auxiliary plasma heating. Although energetic ions from any source contribute to the fusion reactions, the principal source is from Neutral Beam Injection (NBI) hence the designation "beam-target". Depending on the exact plasma parameters and configuration of the heating systems, the contribution of the beam-target reactions can vary significantly and may even constitute the majority of the total fusion reactivity.

The JET tokamak in its latest configuration was equipped with a combination of NBI and Ion Cyclotron Resonance Heating (ICRH) which both produced a fast ion population in the plasma, therefore the beam-target component of the total fusion power has always been significant, around 50% depending on the plasma scenario. In JET DTE2 (2021) the so-called **Tritium-rich** scenario was developed, which was designed to maximize the beam-target reactivity to reach the highest total fusion power [2]. This scenario also demonstrated sustained plasma with high fusion power generated during the target 5 seconds duration. The total fusion energy produced in the most successful pulse was E_{fus}=59MJ, which at the time was the highest fusion energy produced in a single controlled nuclear fusion experiment.

The final D-T campaign at JET (DTE3) took place in 2023. Even though demonstration of high fusion power was no longer the main goal of the experiments [3], a few more Tritium-rich pulses were executed and even higher fusion power output achieved, with E_{fus}=69MJ energy released in a single pulse #104522 and <Q>~0.36 (see Figure 1). The main motivation for repeating the experiments was to support Volumetric Neutron Source (VNS) physics studies which were initiated by EUROfusion in 2022-2023 [4]. VNS concept is similar to the principles of the T-rich scenario: achieve high beam-target reactivity in a relatively small plasma volume which is otherwise not capable of sustaining high thermonuclear reactivity. That machine should be able to achieve DEMO-relevant neutron fluences on the first wall at low construction cost and tritium

consumption rate, therefore can be used to test critical fusion reactor components prior to building a full-scale demonstration plant.

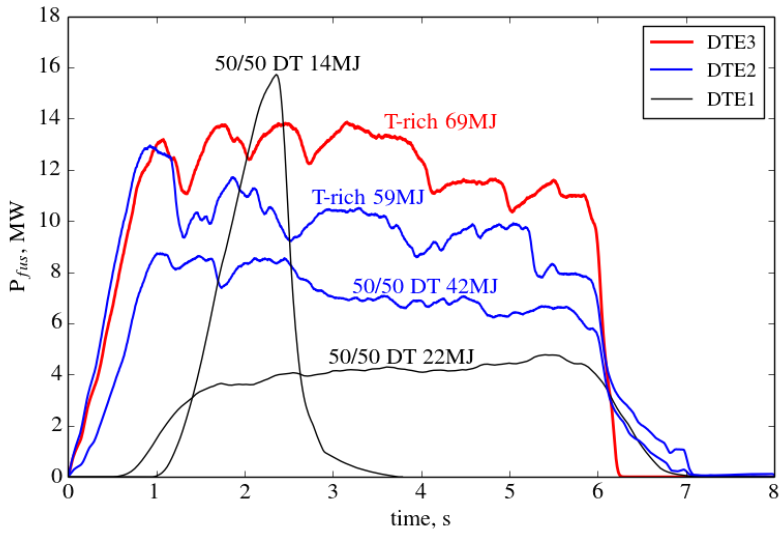

Figure 1: Examples of P_{fus} time traces from different DT campaigns at JET

This paper is organized as follows: section 2 gives a brief overview of the Tritium-rich scenario concept and its efficiency of fusion power generation, section 3 summarizes the experience with Tritium-rich pulses completed in DTE2 and describes motivation for further studies, in section 4 the outcomes of the latest experiment in DTE3 are described, section 5 is dedicated to the discussion of the results and conclusions will be follow in section 6.

2. Tritium-rich scenario.

Development of the Tritium-rich scenario for DTE2 is described in [2]. The main idea behind the scenario is to sustain a population of energetic deuterium ions in a plasma composed mainly of tritium to maximize the number of D_{fast}->T reaction targets. The main source of fast D ions is NBI heating, which is supported by ICRH at the fundamental harmonic D resonance.

Fusion power generation efficiency in such a plasma is determined by a balance between fast ion slowing down via Coulomb collisions with the background plasma ions and electrons and the probability of fusion reaction. The first one can be calculated using the Stix formula [5]:

$$< \frac{dW}{dx} >= -\frac{\alpha}{W} - \beta W^{1/2} \quad (1)$$

Here W is the energy of the fast ion, the first term on the right side represents ion collisions $\alpha=n_e*f(A_i,Z_i)$, A_i and Z_i being mass and charge number of plasma ions and the incident fast ions, and the second term – electron collisions $\beta=n_e*f(1/T_e^{3/2})$. dW/dx represents the energy loss of the fast ion after travelling the distance *dx*. At the same

time, fast deuterium ions travelling distance *dx* through tritium plasma may release fusion energy, with the average expected value of:

$$< \frac{dE_{fus}}{dx} >= n_T * \sigma_{DT}(W) * 17.6MeV \quad (2)$$

where n_T is the density of target tritium ions and $\sigma_{DT}(W)$ is the reaction cross-section as a function of the fast deuterium ion energy. $\sigma_{DT}(W)$ is available in literature, for example in [6] and is shown in figure 2a. Integration of $<dE_{fus}/dx>$ over the whole slowing down trajectory will give the total expected fusion energy from fast ion injected into plasma $<E_{fus}>$, and the ratio of that value to the initial ion injection energy will be the fusion power generation efficiency:

$$Q(E_{inj}, T_e) = \frac{<E_{fus}>}{E_{inj}} = \frac{1}{E_{inj}} * \int_{W=E_{inj}}^{0} < \frac{dE_{fus}}{dx} > * \frac{1}{<dW/dx>} dW \quad (3)$$

Calculated Q values for D-NBI injection into a pure tritium plasma for different T_e values are shown on figure 2b. As the D-T reaction cross-section has a distinct maximum at ~110keV, Q value also shows a maximum around 150-250keV and increases with the electron temperature as the electron collision term in the equation (1) becomes weaker.

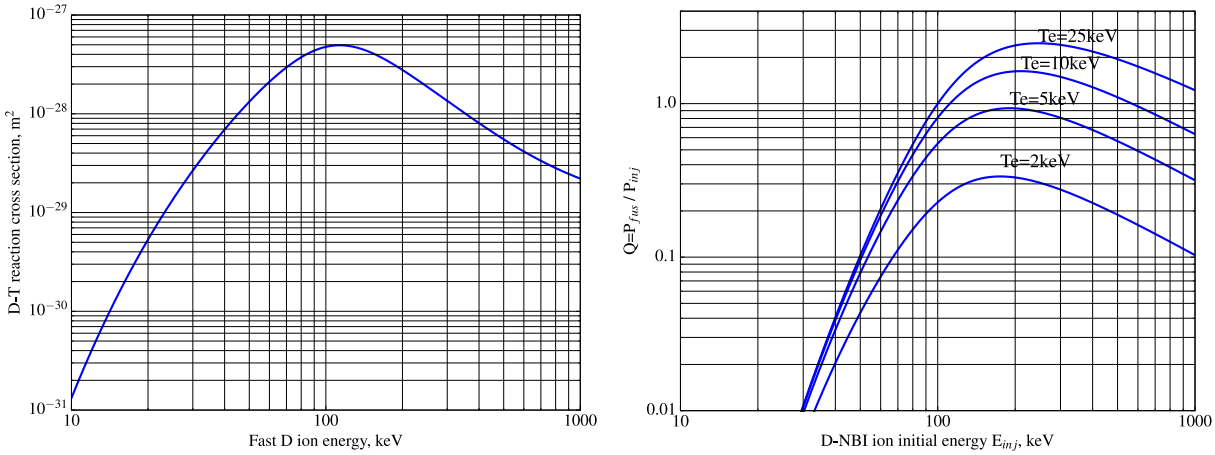

Figure 2: a) cross-section of D-T reaction versus energy of the incident particle (D), with T at rest. b) Beam-target fusion power generation efficiency for the case of D-NBI heating of a pure tritium plasma at different electron temperatures.

Note that even at very high electron temperatures and optimal injection energy, the efficiency is only around Q~2.5 which is too low for a purely beam-target fusion power plant.

JET NBI heating system [7] injects D ions at three energy fractions: 110keV (full energy), 55keV (half energy) and 36keV(one-third) at ratios approximately 0.53/0.34/0.13. As one can see from the figure 2b, the vast majority of the beam-target fusion reactivity comes from the full energy ions; beam-target efficiency for the half-energy fraction is only ~15% of that at the full-energy and the 1/3rd part can practically be ignored.

As the beam target fusion efficiency depends on the local electron temperature at the location of the fast ions, the NBI power deposition profile in plasma has an important role. Plasmas with lower density at the edge are more favourable as the neutral beam penetrates deeper into the plasma where electron temperatures are higher. The JET NBI system consists of two identical beamlines with 8 individual injectors each. Some of these injectors are aligned off-axis with respect to the magnetic centre of the plasma, so part of the injected beam power is not even aimed at the very core. In figure 3, power deposition profiles of all three energy fractions are shown for the record fusion power pulse #104522. One can see that the centre or mass of NBI power deposition for the main energy fraction is located at r/a~0.4 where the electron temperature is around Te~6keV. After summing up the contribution to beam-target reactions of all energy fraction at this electron temperature, we find that the expected fusion power generation efficiency for a pure tritium plasma with no impurities would be **Q~0.43**, which is close to the experimental value of Q~0.38 at the higher performance phase of the record discharge. It should be noted that this number mainly characterizes the configuration of the heating system implemented at JET. With a more optimal alignment of the individual NBI injectors and more power in the primary energy fraction injected, the achievable Q number could be significantly higher, up to Q~0.8.

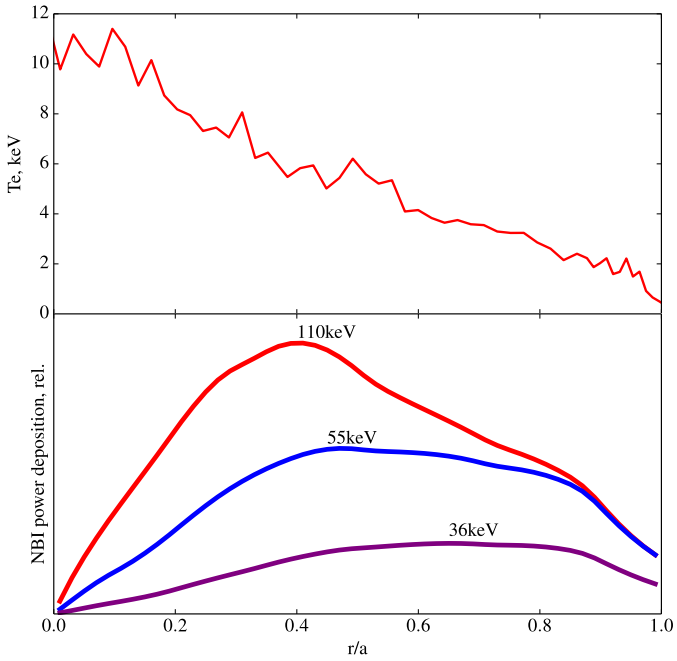

Figure 3: top: electron temperature profile measured with Thomson scattering in the discharge #104522; bottom: NBI power deposition profile for three energy fractions.

In the T-rich scenario at JET, ICRH heating at the fundamental harmonic deuterium resonance was also implemented which additionally interacted with the fast ions, delaying their slowing down or even accelerating them beyond the initial injection energy of 110keV. Calculating the fusion power generation efficiency for ICRH in these

conditions is more complicated and can be found e.g. in [8-9], in general it has similar capacity to that potentially achievable by NBI heating, Q_{ICRH}~0.6-0.7

3. DTE2 outcomes and motivation for further experiments

The Tritium-rich beam-target dominant fusion scenario has been successfully demonstrated at JET during DTE2 (2021) campaign and produced record 59MJ of fusion energy in a single plasma pulse, with $<P_{fus}>$=10.1MW over 5 seconds. Although, maintaining high fusion performance over the whole main heating phase of the discharges was not always possible. Every T-rich pulse where the maximum NBI heating P(NBI)~30MW has been reached, plasmas suffered from core tungsten accumulation and degradation of performance after around 2 seconds of the heating flattop. Therefore, the maximum fusion power P_{fus}~12.5MW in this scenario could not be sustained for the target 5 second duration.

Present day tokamaks with strong NBI heating usually exhibit high toroidal rotation and peaked density profiles, due to the injection of particles and torque. These conditions are very unfavourable for tokamaks with tungsten wall as the neoclassical transport may result in strong compression of heavy impurities to the very core of the plasma [10]. This in turn may lead to a local negative power balance when the radiative losses from the plasma centre exceed the amount of additional heating deposited there, which leads to plasma cooling, reduction of local temperature gradients, suppression of turbulent transport and then even stronger inward convection of tungsten. This process is therefore self-amplifying and leading to eventual discharge termination.

Such conditions are specific to medium-size tokamaks and not expected to be encountered in ITER or fusion power plants due to much lower relative core particle source and injected torque [1]. Construction of a beam-target driven fusion machine for qualification of essential DEMO components (mainly the tritium breeding blankets) is now being re-considered as a vital step to the commercialisation of fusion power [4,11]. Fusion power in such a device will be generated in a manner that is very similar to that demonstrated in the T-rich scenario at JET, with similar concerns over core impurity accumulation. Therefore, additional experiments were performed during DTE3 to address specifically the resilience of plasma to core tungsten accumulation observed when NBI power exceeded a threshold of around 26-28MW.

As the amount of experimental time in DTE3 for the T-rich experiment was very limited, the experimental strategy had to be focussed on a single approach. It was decided to prioritize the effort on achieving the maximum possible ICRH power coupled to this scenario, as it plays an important role in suppressing the tungsten accumulation in these conditions by enhancing the turbulent transport and reducing the plasma density gradients in the core. The role of the magnitude of ICRH power in maintaining of the plasma sustainability in the T-rich scenario has not been studied in DTE2, but the effect

of ICRH modulation on the impurity accumulation was very evident in the power modulation experiment conducted to demonstrate the alpha-heating [12]. Plasma in the DTE3 version of T-rich scenario was moved by 1cm closer to the ICRH antenna to improve the coupling, and more importantly an extensive conditioning of transmission lines was performed prior to the experiment which allowed the system to run at higher values of strap voltage, up to 38kV (typical maximum voltage was 30kV). This proved to be technically successful as the ICRH power coupled to plasma has reached P(ICRH)=5.5MW as opposed to 3.8MW in DTE2, nearly 40% increase.

4. T-rich scenario results in DTE3

The T-rich scenario was immediately reproduced in DTE3 on the first attempt in which full power was available and confirmed its robustness to machine conditions. As the DTE3 campaign was already executed with full NBI heating in deuterium, additional work in changing the species in one of the beamlines as performed in DTE2 was not necessary. Three high-power pulses were performed in DTE3, each of which produced more fusion energy than the previous record value of 59MJ in DTE2. Maximum NBI power of 30MW was once again reached, similar to that of DTE2, but it was made with fewer individual injectors (14 versus 15) which were run at slightly higher energy. A summary of the pulses can be found in table 1 and the overview of the time traces in figure 4.

Pulse number	Efus, MJ	P(NBI)	P(ICRH)
104520	63	28MW	4.8MW
104675	66	28MW	5.5MW
104522	**69**	**30MW**	**5.5MW**

Table 1: summary of high fusion power T-rich pulses performed in DTE3

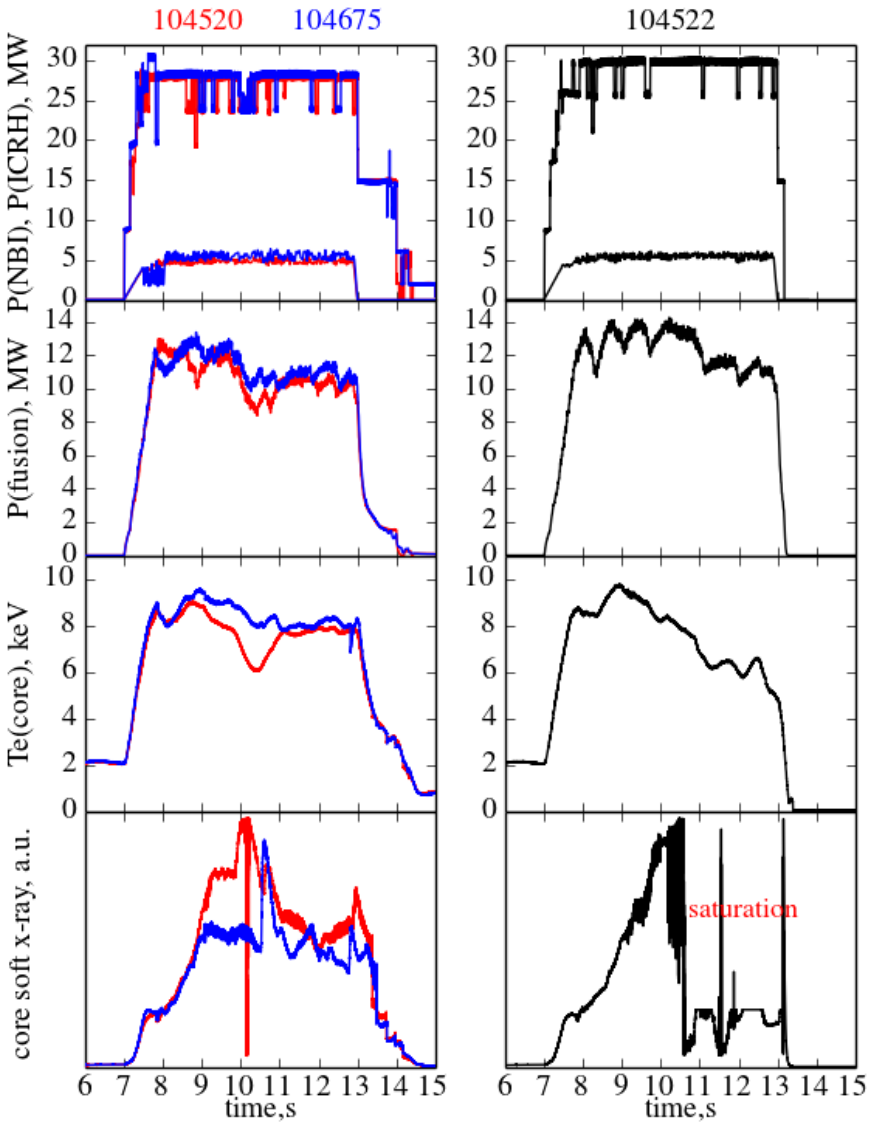

Figure 4: overview of three T-rich pulses performed during DTE3. left: 104520 and 104675, sustained with no evidence of core impurity content growth; right: the highest E_{fus}=69MJ pulse 104522 with slow impurity accumulation.

Overall reliability of the NBI power was improved since DTE2 and the heating power levels were a lot more stable over the whole heating window. Two pulses were run with 13 NBI injectors resulting in 28MW of P(NBI) power and did not exhibit the avalanche of tungsten accumulation in the core, despite that one of the pulses had somewhat lower ICRH power (see table 1). The pulse with the highest injected NBI power, #104522 achieved the highest fusion energy yield of 69MJ but showed impurity accumulation triggered at around 2 seconds after the start of the main heating phase, therefore repeating the results of DTE2 pulse #99972 with similar P(NBI)=30MW power [2]. Additional P(ICRH) in T-rich scenario achieved in DTE3 did not prevent core tungsten accumulation and consequent discharge degradation in the record pulse but slowed it down sufficiently to demonstrate high fusion power over the desired 5 seconds

duration. Note that (see figure 3) the majority of NBI power in these discharges is deposited off-axis, therefore the effect of the core plasma cooling on the total beam-target fusion power is somewhat delayed until the affected plasma volume becomes sufficiently large.

5. Discussion of the results.

Tritium-rich experiments in DTE3 with better reproducibility and stability of delivered NBI power have confirmed the conclusions of DTE2: for this scenario there is an apparent threshold in the NBI power of around 28MW which triggers core tungsten accumulation and eventual degradation of the discharge's performance. Significant increase in P(ICRH) did not change the threshold and did not delay the core temperature roll-over. Some additional physics must play a role at the time of the impurity accumulation trigger around t_{heat}+2s.

The T-rich scenario used in this work has been adapted from the hybrid scenario developed for the 50/50 D/T case [13]. It retained the pre-tailoring of the q-profile prior to the H-mode entry to a shape with a broad low shear area in plasma core with central q_0>1. The q-profile then evolved throughout the heating phase, with first fishbones typically appearing at ~t_{heat}+2s. The following evolution of the q-profile depends on the core electron temperature [2]. If impurity accumulation and core radiation is growing, then due to plasma cooling and increased resistivity near the magnetic axis the core q_0 value start to increase again and the fishbones disappear. If the accumulation was avoided and the electron temperature profile remained peaked, then q_0 decreases further with continuous n=1 mode appearing later in the discharge and eventual sawtooth crash happening near the end of the main heating phase.

As the q-profile evolves, the time traces of the electron temperature from the Electron Cyclotron Emission (ECE) in these plasmas also demonstrate changes in behaviour. All high-performance T-rich pulses around t_{heat}+1.1-1.5s show sudden increase in the core electron temperature gradient, seen as a difference between the measured Electron Cyclotron Emission (ECE) signals from r/a~0 and r/a~0.3 radial positions. The change is always happening before the start of the fishbones activity. Similar behaviour has been observed in JET hybrid scenarios before (see figure 5) and has been reported in [14]. It was associated with triggering of Internal Transport Barrier (ITB) at q=1 surface.

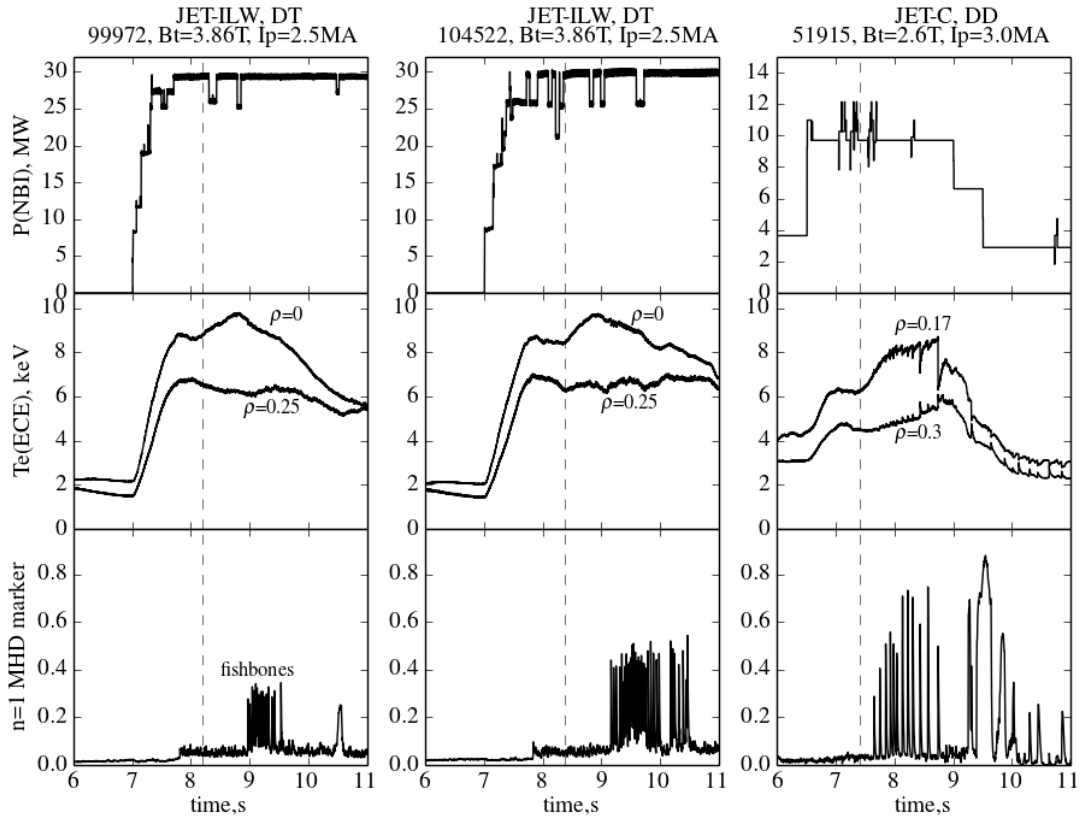

Figure 5: similar ITB phenomena observed in JET at different times; left: #104522 in DTE3 (2023), right: #51915 in JET-C (2000). ECE time traces are taken from different radial coordinates for two cases as the line of sight of the diagnostic has changed between 2000 and 2023.

The core soft x-ray emission grows rapidly during the ITB phase and either stabilizes soon after the core temperature reaches maximum (figure 4 left) or continues to rise (figure 4 right) until the measurement is saturated. In the latter case the core impurity accumulation and plasma central cooling is triggered.

Prior to the DTE3 campaign, the High-Resolution Thomson Scattering diagnostic (HRTS) [15] has been realigned to the very core area of plasma and provided measurements down to r/a~0 instead of r/a>0.2 available previously. Therefore, Thomson Scattering profiles for the core ITB in the latest T-rich pulses become available in addition to ECE time traces and are shown on figure 5 for the pulse 104522. The location of the ITB foot at r/a~0.3 visible both on T_e and n_e profiles. Unfortunately, the ion temperature measurements in these pulses in the very core area are not sufficiently accurate to conclude if the transport improvement also affects the ion channel. TRANSP [16] simulations were performed for this discharge and showed significant reduction of the electron heat transport inside r/a=0.3 during the ITB phase.

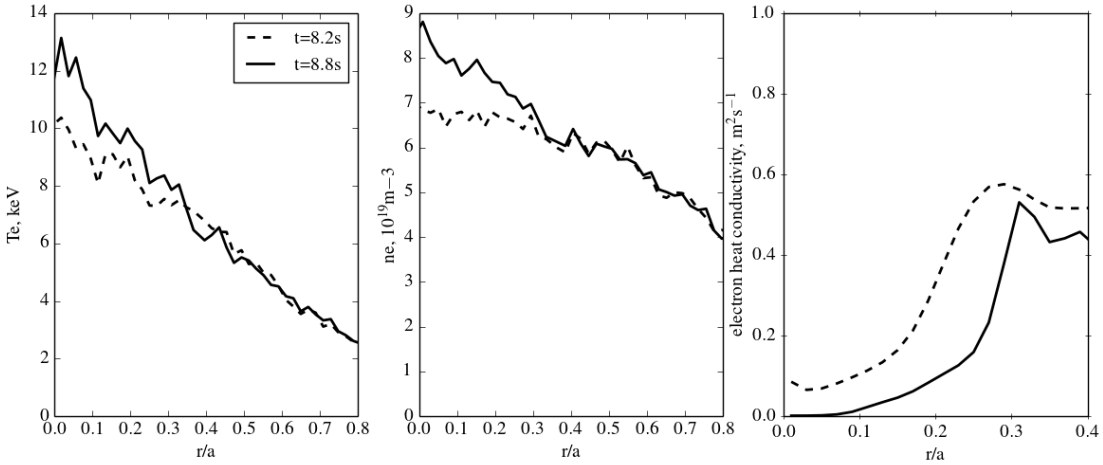

Figure 6: left+middle: Thomson scattering Te and ne profiles in the highest fusion energy shot 104522, before and after core ITB formation. Right: electron heat conductivity, χ_e reconstructed with TRANSP code [16].

Transport of heavy impurities in tokamaks has been subject of numerous studies for almost two decades [10,17]. In the core part of the plasma, tungsten transport is dominated by collisional effects (neoclassical transport) which in presence of a peaked density profile and high rotation velocity typically causes strong inward pinch [18]. Even in the presence of the neoclassical pinch, catastrophic tungsten accumulation could be avoided by sufficiently strong turbulent transport in the core area. Application of central ICRH or ECRH heating has been recognized as an effective way to suppress tungsten accumulation in NBI heated highly rotating plasmas [19,20], as it serves three goals:

- Localized electron heating helps to maintain positive power balance in the presence of tungsten.
- Increases the intensity of the turbulent transport as more energy needs to be transported outwards, thus amplifying its effect on tungsten.
- Intense turbulent transport reduces local density gradients produced by NBI particle deposition, thus reducing the neoclassical impurity pinch itself.

The balance between collisional and turbulence effects on tungsten transport can be affected by the presence of mechanisms which cause reduction or suppression of plasma turbulence, observed in tokamaks in the form of Internal Transport Barriers. It has indeed been suggested in theoretical studies [21] and observed experimentally on JET [22] and more recently on EAST [23]. That explains the observations of tungsten accumulation in the T-rich scenario in DTE2 and DTE3 campaigns, namely the correlation between the core ITB formation and the timing of the start of the accumulation as well as inefficiency of additional ICRH power on the ability to avoid it.

Once the T-rich discharge goes past the ITB phase around t_{heat}+2s without excessive amount of tungsten penetrated in the core, it seems to remain resilient to tungsten

accumulation as even a strong transient impurity event observed in 104675 at around t=10.5s (figure 4) did not ultimately affect the performance as the injected impurities were eventually expelled. It is worth noting that the sustained pulses exhibit significant core n=1 MHD activity after the ITB phase, which may contribute to the tungsten accumulation avoidance. That unfortunately cannot be proven as in all the pulses with impurity accumulation n=1 MHD activity was not present due to elevated $q_0>1$ which was the result of the cooling of the plasma core.

6. Conclusions

The Tritium-rich scenario developed at JET in the 2nd DT campaign has been reproduced in DTE3. Three plasma pulses were done, each of which produced more fusion energy than the highest performing pulse in DTE2. The best performing pulse 104522 achieved a fusion yield of E_{fus}=69MJ in the whole pulse and $<P_{fus}>$=12.4MW over a 5 second window, which is 2.3 MW more than the previous record pulse #99971 in DTE2.

The main difference between DTE2 and DTE3 experiments was in the level of coupled ICRH power, which was increased by up to 40%. The motivation for that was to demonstrate improved resilience to high-Z impurity accumulation routinely observed in DTE2 pulses in plasmas where maximum available P(NBI)~30MW was delivered. This was partially successful, as the pulse 104522 with P(NBI)~30MW did achieve the highest fusion yield. Nonetheless, the impurity accumulation could not be avoided completely but only slowed down sufficiently to extend the high fusion power phase to 5 seconds.

More detailed analysis of the pulses, supported by better diagnostic coverage suggested that the particular T-rich scenario developed at JET was experiencing a transient ITB near the time of the appearance of q=1 surface in the core. The ITB was weak and localised to the very central part of plasma, therefore didn't have a noticeable effect on the plasma total stored energy and fusion power. Nonetheless, it seemed to have had a profound effect on the impurity accumulation which was observed to happen simultaneously. That can explain the inefficiency of the substantial increase of the coupled ICRH power on avoidance of the accumulation.

Detailed modelling of tungsten transport in these conditions is outside of the scope of this paper, but the JET data remains available and will be used in future for validation of tungsten transport modelling for the Volumetric Neutron Source machine [24]

Acknowledgements

This work has been carried out within the framework of the EUROfusion Consortium, funded by the European Union via the Euratom Research and Training Programme (Grant Agreement No 101052200 — EUROfusion) and from the EPSRC [grant number EP/W006839/1]. To obtain further information on the data and models underlying this

paper please contact PublicationsManager@ukaea.uk. Views and opinions expressed are however those of the author(s) only and do not necessarily reflect those of the European Union or the European Commission. Neither the European Union nor the European Commission can be held responsible for them.

References

[1] A. Loarte *et al* 2025 *Plasma Phys. Control. Fusion* **67** 065023
[2] M. Maslov *et al* 2023 *Nucl. Fusion* **63** 112002
[3] A. Kappatou *et al 2025 Plasma Phys. Control. Fusion* **67** 045039
[4] C. Backmann et al Fusion Engineering and Design 211 (2025) 114796
[5] T. H. Stix 1972 Plasma Physics 14 367
[6] NRL Plasma Formulary https://www.nrl.navy.mil/News-Media/Publications/nrl-plasma-formulary/
[7] D B King *et al* 2025 *Plasma Phys. Control. Fusion* **67** 095017
[8] E Lerche et al., *AIP Conf. Proc.* 2984, 030005 (2023)
[9] E Lerche et al., Nucl. Fusion to be published 2025
[10] C. Angioni 2025 *Nucl. Fusion* **65** 062001 **DOI** 10.1088/1741-4326/add1ee
[11] Gianfranco Federici 2023 *Nucl. Fusion* **63** 125002
[12] P. Mantica *et al* 2024 *Nucl. Fusion* **64** 086001
[13] J. Hobirk *et al* 2023 *Nucl. Fusion* **63** 112001
[14] E. Joffrin et al 2002 Plasma Phys. Control. Fusion 44 1203
[15] L. Frassinetti et al., Rev. Sci. Instrum. 83, 013506 (2012); https://doi.org/10.1063/1.3673467
[16] Breslau J., Gorelenkova M., Poli F., Sachdev J., Pankin A., Perumpilly G., Yuan X. and Glant L. 2018 *TRANSP* (Princeton Plasma Physics Laboratory (PPPL), USDOE Office of Science (SC), Fusion Energy Sciences (FES) (SC-14)) https://doi.org/10.11578/dc.20180627.4
[17] M. Yoshida (Chair Transport and Confinement) *et al* 2025 *Nucl. Fusion* **65** 033001**DOI** 10.1088/1741-4326/ad8ced
[18] C. Angioni et al *Phys. Plasmas* 22, 055902 (2015) https://doi.org/10.1063/1.4919036
[19] C. Angioni *et al* 2017 *Nucl. Fusion* **57** 056015**DOI** 10.1088/1741-4326/aa6453
[20] E. Lerche *et al* 2016 *Nucl. Fusion* **56** 036022**DOI** 10.1088/0029-5515/56/3/036022
[21] T. Fülöp; H. Nordman Phys. Plasmas 16, 032306 (2009) https://doi.org/10.1063/1.3083299
[22] R. Dux et al 2004 Nucl. Fusion 44 260
[23] Wenmin Zhang *et al* 2025 *Nucl. Fusion* **65** 052003**DOI** 10.1088/1741-4326/adcbc1
[24] E. Bray et al to be published